Slowing Heavy, Ground-State Molecules using an Alternating Gradient Decelerator

M. R. Tarbutt,[1] H. L. Bethlem,[2] J. J. Hudson,[1] V. L. Ryabov,[3] V. A. Ryzhov,[3] B. E. Sauer,[1] G. Meijer,[4] and E. A. Hinds[1]

[1]*Blackett Laboratory, Imperial College, London SW7 2BW, United Kingdom*

[2]*FOM-Institute for Plasma Physics Rijnhuizen, P.O. Box 1207, NL-3430 BE Nieuwegein, The Netherlands*

[3]*Petersburg Nuclear Physics Institute, Gatchina, Leningrad 188300, Russia*

[4]*Fritz-Haber-Institut der Max-Planck-Gesellschaft, Faradayweg 4-6, D-14195 Berlin, Germany*

(Received 19 December 2003; published 27 April 2004)

We have decelerated a supersonic beam of ^{174}YbF molecules using a switched sequence of electrostatic field gradients. These molecules are 7 times heavier than any previously decelerated. An alternating gradient structure allows us to decelerate and focus the molecules in their ground state. We show that the decelerator exhibits the axial and transverse stability required to bring the molecules to rest. Our work significantly extends the range of molecules amenable to this powerful method of cooling and trapping.

DOI: 10.1103/PhysRevLett.92.173002 PACS numbers: 33.80.Ps, 33.55.Be, 39.10.+j

It has recently become possible to decelerate cold supersonic beams of light polar molecules in suitable excited states using electrostatic forces. This has been demonstrated with beams of CO [1], ND_3 [2,3], and OH [4]. Once the molecules are sufficiently slow they can be trapped electrostatically [3,5]. The key feature of an electrostatic decelerator is that molecules move through the fringe field of a capacitor from low to high electric field. If the molecules are weak-field seekers the increase in their potential energy causes them to slow down. The field is then switched off and the molecules fly out of the capacitor without being accelerated. With many capacitors along the beam line, this process can be repeated until the molecules are brought to rest. The highest electric fields are on the surfaces of the electrodes, resulting in a transverse force towards the beam axis that focuses the weak-field-seeking molecules as they propagate through the decelerator [3].

Until now, no ground state beam has been decelerated because ground state molecules are strong-field seekers. Strong-field seekers can be decelerated by reversing the charging sequence so that the field is off when the molecules enter each capacitor and switched on before they leave. However, Maxwell's equations prevent the simple focusing that weak-field seekers enjoy because it is not possible to have a static maximum of electric field in free space [6]. This difficulty can be overcome by the method of alternating gradient focusing, whereby a sequence of alternating focusing and defocusing lenses results in a net focusing effect. Recently a beam of strong-field-seeking CO molecules in the metastable $a\,^3\Pi$ state was slowed from 275 to 260 m/s in such a decelerator [7]. Here we report the deceleration and focusing of a supersonic ^{174}YbF beam in the ground state $X\,^2\Sigma^+(v = 0, N = 0)$, and we show that it is feasible to bring such molecules to rest. These are 7 times heavier than any molecules previously decelerated, so the amount of kinetic energy to be removed is proportionally larger. If the number of decelerator stages is to remain practical, each stage must remove a large amount of energy. Much more energy can be removed from heavy molecules in their ground state than in any weak-field-seeking state.

The ability to decelerate heavy molecules and ground state molecules greatly extends the range of species that can be electrostatically slowed and trapped. YbF is of particular interest because it offers one of the most sensitive ways to search for elementary particle physics beyond the standard model through a measurement of the electric dipole moment of the electron [8]. This important quantity can be measured more sensitively by slowing the molecules. Furthermore, deceleration would enhance experiments that study possible connections between the homochirality of biomolecules and parity violation [9,10] and would improve the sensitivity of nuclear anapole measurements [11].

Our beam line is shown in Fig. 1(a). The supersonic source uses 4 bars of Ar, Kr, or Xe mixed with a small fraction of SF_6 as the carrier gas. A solenoid valve releases this gas every 0.2 s in 100 μs pulses that expand

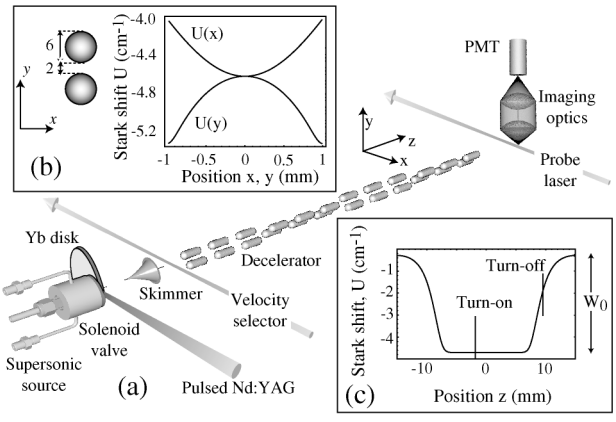

FIG. 1. (a) The beam line. (b) Left: end view of one decelerator stage. Graph: Stark shift of ground state YbF within the stage versus x and y for electrode voltages of ± 10 kV. (c) Same Stark shift versus z, plotted for one stage.

through a nozzle into a vacuum of $\sim 5 \times 10^{-5}$ mbar. A disk of Yb is positioned immediately outside the nozzle. The edge of this disk is ablated by the unfocused 1064 nm output of a 10 ns, 20 mJ pulsed Nd:YAG laser. The Yb and SF_6 react to form YbF, which becomes entrained in the gas pulse and thermalizes with it. The molecules then pass through a 1 mm diameter skimmer, 82 mm from the nozzle, into a high vacuum. This source produces YbF beams as slow as 290 m/s with translational and rotational temperatures as low as 1.4 K [12]. A 552 nm laser beam, the velocity selector, crosses the molecular beam 108 mm downstream from the skimmer. This laser beam pumps molecules out of the ground state except during an adjustable period of typically 10–20 μs when it is switched off. The moment at which a molecule crosses the laser beam is mainly determined by its speed. Consequently, the resulting pulse of ground state molecules is a velocity group whose width and center are determined by the timing of the laser pulse. A further 4 mm downstream the molecules enter the decelerator. This has 12 stages, each comprising a pair of 20 mm long stainless steel rods parallel to the beam axis z and rounded to have hemispherical ends. The rods are 6 mm in diameter, with a 2 mm gap between them, as indicated on the left of Fig. 1(b). The stages are separated from each other by 10 mm gaps. They are arranged in four groups of three, alternating between vertical (y) and horizontal (x) orientation, as illustrated in Fig. 1(a). Finally, a 552 nm probe laser, 258 mm from the end of the decelerator and perpendicular to the molecular beam, selectively excites one hyperfine sublevel of the ground state. The time evolution of the fluorescence is detected by a photomultiplier.

The decelerator electrodes are operated at ± 10 kV, giving an electric field on the axis of nearly 100 kV/cm at the center of each stage. Figure 1(b) shows the resulting Stark shift of the molecules in a vertical stage versus transverse position x or y. This potential focuses the molecules toward the beam axis in the x direction and defocuses them along y. It is approximately harmonic over most of the region between the electrodes. The transverse motion can therefore be described using transfer matrices (as in optics), and the transverse oscillations are stable provided $-2 < \mathrm{Tr}(M) < 2$, where M is the transfer matrix for one unit of the periodic structure [7]. We have chosen to alternate the focusing and defocusing axes after every third lens, rather than between each lens. In this way, we are able to maximize the number of deceleration stages per unit length and still satisfy the alternating gradient stability criterion.

Figure 1(c) shows the variation of the Stark shift along the beam axis through one stage. As the beam pulse passes through the stage the voltages are switched on and off by fast high-voltage switches under the control of a 50 MHz pattern generator. Figure 1(c) illustrates where the field might be switched on and off to decelerate a molecule moving to the right. The switching sequence that decelerates a pulse of molecules through many stages is designed so that a particular molecule, known as the synchronous molecule, reaches the same positions within each stage at the moments of switching on and off. The switch-off position is described by a phase angle ϕ defined through the energy loss of the synchronous molecule per stage $W_0 \sin\phi$, where W_0 is the maximum possible energy loss per stage. By choosing $\phi < 90°$ we ensure that those molecules running ahead of the synchronous molecule are decelerated more, while those lagging behind are decelerated less. This phase stability is important for a decelerator because it allows a finite velocity group of molecules to propagate as a bunch [13].

The dotted curve in Fig. 2(a) shows the YbF time-of-flight distribution with the decelerator off, using Xe carrier gas precooled to 210 K. We deduce from this distribution that the YbF pulse has a mean velocity of 298 m/s distributed with a full width at half maximum (FWHM) of 26 m/s, corresponding to a temperature of 2.7 K. When the decelerator is turned on (solid line) at a phase angle of 60°, approximately half the molecules gather into a narrow bunch whose speed is 287 m/s with 13 m/s FWHM. Most of the molecules inside the bunch have been decelerated, although some of the slowest molecules from the original distribution are accelerated into the bunch, as indicated by the reduction in the number of molecules at long arrival times when the decelerator is turned on. The bunch will stay together as more stages of deceleration are added to bring it to rest.

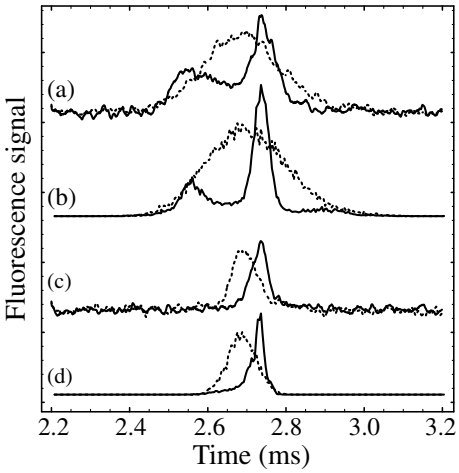

FIG. 2. Time-of-flight profiles for 298 m/s YbF beams with decelerator off (dotted lines) and on (solid lines). The time origin is defined by the Nd:YAG pulse. (*a*) Experiment using the whole pulse of molecules. (*b*) Simulation for (*a*). (*c*) Experiment using a velocity-selected pulse of molecules. (*d*) Simulation for (*c*). The vertical axes of the simulations are scaled to account for transverse focusing, which is not otherwise included.

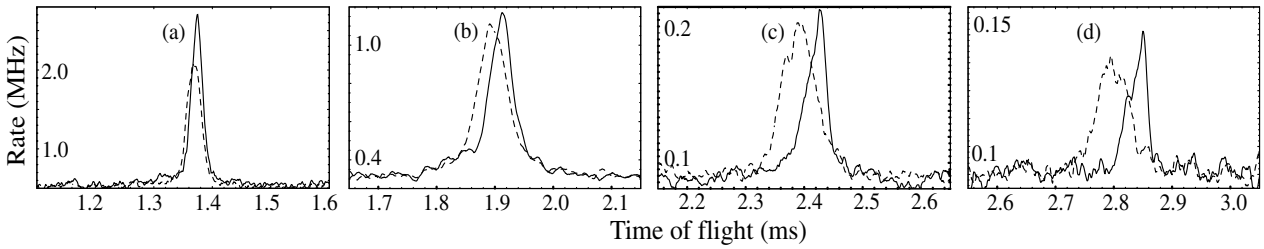

FIG. 3. Deceleration of YbF beams from various initial speeds. Dotted (solid) lines show time-of-flight profile with decelerator off (on). The y axes indicate the fluorescence rates in the detector. (a) YbF in Ar. $v_i = 586.3 \pm 1.0$ m/s, $\Delta v = 5.1 \pm 0.9$ m/s, $\Delta E = 48.1 \pm 8.7$ cm^{-1}. (b) YbF in Kr. $v_i = 421.8 \pm 0.7$ m/s, $\Delta v = 6.9 \pm 0.7$ m/s, $\Delta E = 46.8 \pm 4.8$ cm^{-1}. (c) YbF in Xe. $v_i = 335.1 \pm 0.5$ m/s, $\Delta v = 9.3 \pm 0.5$ m/s, $\Delta E = 50.0 \pm 2.4$ cm^{-1}. (d) YbF in Xe cooled to 198 K. $v_i = 286.5 \pm 0.5$ m/s, $\Delta v = 10.2 \pm 0.4$ m/s, $\Delta E = 46.6 \pm 2.1$ cm^{-1}.

To test our understanding of the decelerator, we simulate the motion of molecules through the apparatus by integrating the axial equation of motion using the calculated potential on the axis of the beam line, which is plotted in Fig. 1(c). For the initial velocity distribution in the simulation, we take a beam whose temperature and central velocity have the values derived from the dotted data in Fig. 2(a). The result of this calculation, plotted in Fig. 2(b), is qualitatively very similar to the experimental result, indicating that the motion of the molecules is indeed roughly separable into axial and transverse components and showing that we understand the basic deceleration process.

Figure 2(c) shows the results obtained with the velocity selector turned on and timed to select the central 20 μs section of the pulse. The resulting velocity distribution remains centered on 298 m/s but now has a FWHM of only 8.5 m/s. When the decelerator is turned on, this entire distribution is shifted down in velocity by 10 m/s, and the time-of-flight profile is narrowed to 70% of its original width because the decelerator slows down the faster molecules in the bunch more than the slower ones. Figure 2(d) confirms that these results are also well described by a simple simulation of the axial motion.

We have further tested the decelerator using four other initial speeds, chosen by varying the mass and temperature of the carrier gas, with the results shown in Fig. 3. In each experiment the velocity selector was used to narrow the velocity distribution to a FWHM in the range 9–14 m/s. This longitudinal velocity range lies within the phase stability range of the decelerator, meaning that the entire velocity-selected pulse can be decelerated. In all four experiments, the phase angle is set to 60°, corresponding to a total energy loss of 46 cm^{-1}. The measured energy loss confirms this, showing that the decelerator works correctly over a wide range of initial speeds. All the beams become 20%–30% narrower in their time-of-flight profile when the decelerator is switched on as a result of the phase stability. The slowest beam we have produced is shown in Fig. 3(d). Here the speed of the molecules entering the decelerator is only 286.5 m/s, and the decelerator reduces their energy by 7%.

The final speed of the molecules can be adjusted by making an appropriate choice of phase ϕ in the high-voltage switching pattern, as shown by the data points in Fig. 4. Here we have simply taken the peak of the decelerated pulse as a measure of the speed. The solid line shows the expected change for a synchronous molecule, corresponding to an energy loss of $W_0 \sin\phi$ per stage. Crosses show the result of a numerical simulation that takes into account the entire ensemble of molecules. The uncertainty in these simulations is the same as the error bars on the data. As the phase is increased toward 90°, the measured change of speed shows reasonable agreement with the theories. Figures 2–4 show that this alternating gradient decelerator works well over a wide range of operating parameters and that its deceleration and phase stability properties are well understood.

Transverse confinement is important for the successful operation of the decelerator. In order to study this experimentally we measured the number of molecules reaching the detector for a range of electrode voltages and lens lengths. Although the physical length of the electrodes is fixed, we can vary the length of time for which each lens acts on the molecules by changing the turn-on point in the timing sequence [Fig. 1(c)], keeping the turn-off point

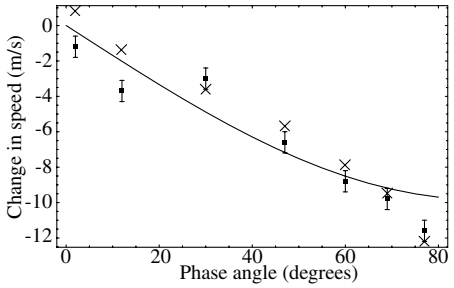

FIG. 4. Change in speed of molecules versus decelerator phase angle for a beam of initial speed 335 m/s. Points: Measured data. Solid line: Simple theory for synchronous molecule. Crosses: Numerical simulation.

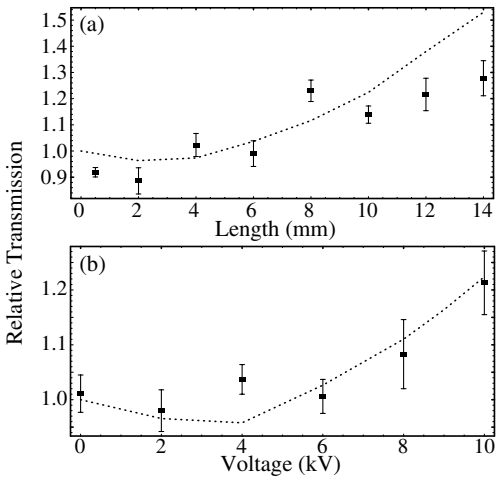

FIG. 5. Normalized decelerator transmission versus (a) effective lens length at a voltage of ± 10 kV, and (b) electrode voltage for a fixed lens length of 10 mm. Dotted lines: calculation using matrix approach.

fixed. Measurements on a 590 m/s beam are shown in Fig. 5, where we plot the total number of molecules transmitted through the decelerator, normalized to the number when the decelerator is off for various lens lengths [5(a)] and various electrode voltages [5(b)]. The dotted lines show the expected transmission of molecules through our decelerator in the absence of edge effects, lens aberrations, and misalignments. This was calculated using transfer matrices, sampling over a realistic range of initial transverse velocities and positions. At low lens power, the calculated transmission dips below unity because the defocusing lenses are 10% stronger than the focusing ones. At higher power, alternating gradient focusing increases the transmission. Our data follow the expected trend, whereas the only previous study of alternating gradient deceleration of molecules showed a 20-fold shortfall in the transmission, a problem attributed to misalignments of the electrodes [7]. By varying the phase angle ϕ we can control the fraction of time that the molecules spend in the fringe fields of the lenses, and we find that this alters the focusing. We believe that the fringe fields, not accounted for in the matrix model, are the cause of the small discrepancy between theory and experiment observed in Fig. 5(a). This observation underlines the importance of keeping the fringe fields under review while designing alternating gradient decelerators.

We have demonstrated that heavy ground state molecules can be slowed down by using an alternating gradient decelerator. The technique we have demonstrated can be applied to a wide range of heavy polar molecules. We have used a 12-stage decelerator operated at a field of 100 kV/cm with a deceleration phase angle of 60° to remove 7% of the kinetic energy of YbF molecules. We were able to raise the electric field to 140 kV/cm without electric field breakdown. At this higher field, 110 stages would bring the molecules to rest. They could then be coupled into an electrodynamic trap [14,15] or a wire trap [16], or they could be switched into a weak-field seeking state and stored in an electrostatic trap, e.g., a quadrupole trap [17] or chain-link trap [18]. Trapping heavy molecules will provide a spectacular increase in the spectroscopic resolution available, leading to new applications in metrology, quantum chemistry, and fundamental physics.

We are indebted to Henrik Haak and André van Roij for mechanical design work and to Victor Ezhov for valuable discussions. This work was supported in the UK by PPARC, EPSRC, and JIF, by the EU "Cold Molecules" network, and in Russia by RFBR Grant No. 02-02-17090. H. L. B. acknowledges support from the NWO.

[1] H. L. Bethlem, G. Berden, and G. Meijer, Phys. Rev. Lett. **83**, 1558 (1999).
[2] H. L. Bethlem *et al.*, Nature (London) **406**, 491 (2000).
[3] H. L. Bethlem, F. M. H. Crompvoets, R. T. Jongma, S. Y. T. van de Meerakker, and G. Meijer, Phys. Rev. A **65**, 053416 (2002).
[4] J. R. Bochinski, E. R. Hudson, H. J. Lewandowski, G. Meijer, and J. Ye, Phys. Rev. Lett. **91**, 243001 (2003).
[5] F. M. H. Crompvoets, H. L. Bethlem, R. T. Jongma, and G. Meijer, Nature (London) **411**, 174 (2001).
[6] W. H. Wing, Prog. Quantum Electron. **8**, 181 (1984).
[7] H. L. Bethlem, A. J. A. van Roij, R. T. Jongma, and G. Meijer, Phys. Rev. Lett. **88**, 133003 (2002).
[8] J. J. Hudson, B. E. Sauer, M. R. Tarbutt, and E. A. Hinds, Phys. Rev. Lett. **89**, 023003 (2002).
[9] Ch. Daussy *et al.*, Phys. Rev. Lett. **83**, 1554 (1999).
[10] M. Ziskind, C. Daussy, T. Marrel, and Ch. Chardonnet, Eur. Phys. J. D **20**, 219 (2002).
[11] D. DeMille (private communication).
[12] M. R. Tarbutt *et al.*, J. Phys. B **35**, 5013 (2002).
[13] H. L. Bethlem, G. Berden, A. J. A. van Roij, F. M. H. Crompvoets, and G. Meijer, Phys. Rev. Lett. **84**, 5744 (2000).
[14] F. Shimizu and M. Morinaga, Jpn. J. Appl. Phys. 2 **31**, L1721 (1992).
[15] E. Peik, Eur. Phys. J. D **6**, 179 (1999).
[16] S. K. Sekatskii and J. Schmiedmayer, Europhys. Lett. **36**, 407 (1996).
[17] W. H. Wing, Phys. Rev. Lett. **45**, 631 (1980).
[18] N. E. Shafer-Ray *et al.*, Phys. Rev. A **67**, 045401 (2003).